Electronic Supplementary Material (ESI) for Dalton Transactions.

Supporting Information

Post-functionalization of a Photoactive Hybrid Polyoxometalate

Jamie M. Cameron, Satomi Fujimoto, Rong-Jia Wei, Graham N. Newton,* and Hiroki Oshio*

Experimental Section

Syntheses and Materials

All reagents were obtained from commercial sources and were used without further purification.

The ligand 4-carboxyphenyl phosphonic acid[1] and the hybrid polyoxometalate $K_6[P_2W_{17}O_{61}(P(=O)C_6H_5COOH)_2]\cdot6C_4H_9NO$ (**1**) were prepared by reported methods.[2]

$K_4H_6[Zn(H_2O)_2(P_2W_{17}O_{61}(P(=O)C_6H_5COOH)_2)_2]\cdot8C_4H_9NO\cdot9CH_3CN$ (**2**) : **1** (99.8 mg, 0.020 mmol) and $Zn(NO_3)_2\cdot6H_2O$ (55.3 mg, 0.19 mmol) were dissolved in acetonitrile : water (6 : 1 (v/v)) solution and then filtered. Evaporation of the mixture at room temperature for 1 week gave pale green crystals of **2** for the X-ray diffraction analysis. Yield: 12.9 mg (13 % based on W)

^1H NMR (DMSO-*d*$_6$, 400 MHz): 7.98 (dd, 8H), 8.12 (dd, 8H). ^{31}P NMR (DMSO-*d*$_6$, 400 MHz): 13.30, -11.35, -12.92. IR (KBr): 1692 (s, $\nu_{C=O}$), 1601 (s, $\nu_{C=C}$), 1404 (m, $\nu_{C=C}$), 1092 (s, $\nu_{W=O}$), 1036 (s, $\nu_{W=O}$), 962 (s, $\nu_{W=O}$), 908 (s, $\nu_{W=O}$), 816 (s, $\nu_{W=O}$) cm^{-1}. Elemental analysis; $C_{78}H_{129}K_4N_{17}O_{144}P_8W_{34}Zn$ calc. K 1.5, H 1.3, C 9.1, N 2.3; found K 1.5, H 1.2, C 9.4, N 2.4.

$K_4H_6[Co(H_2O)_2(P_2W_{17}O_{61}(P(=O)C_6H_5COOH)_2)_2]\cdot12C_4H_9NO\cdot3CH_3CN$ (**3**): The procedure is similar to the synthesis of **2**. **1** (103.0 mg, 0.02 mmol) and $Co(NO_3)_2\cdot6H_2O$ (58.0 mg, 0.20 mmol) were dissolved in acetonitrile : water (6 : 1 (v/v)) solution and filtered. Evaporation of the mixture at room temperature for 1 week gave pale orange crystals of **3** for the X-ray diffraction analysis. Yield: 11.4 mg (11 % based on W)

IR (KBr) : 1695 (s, $\nu_{C=O}$), 1605 (s, $\nu_{C=C}$), 1404 (m, $\nu_{C=C}$), 1092 (s, $\nu_{W=O}$), 958 (s, $\nu_{W=O}$), 918 (s, $\nu_{W=O}$), 822 (s, $\nu_{W=O}$) cm^{-1}. Elemental analysis; $C_{82}H_{147}CoK_4N_{15}O_{148}P_8W_{34}$ calc. K 1.5, H 1.4, C 9.5, N 2.0; found K 1.4,H 1.3, C 9.4, N 1.8.

$(Mn(H_2O)_6)K_3H_5[Mn_2(OH)_2(H_2O)_4(P_2W_{17}O_{61}(P(=O)C_6H_5COOH)_2)_2]\cdot3C_4H_9NO\cdot17CH_3CN$ (**4**): The procedure is similar to the synthesis of **2**. **1** (100.6 mg, 0.020 mmol) and $Mn(NO_3)_2\cdot6H_2O$ (57.4 mg, 0.20 mmol) were dissolved in acetonitrile : water (6 : 1 (v/v)) solution and filtered. Evaporation of the mixture at room temperature for 1 week gave pale yellow crystals of **4** for the X-ray diffraction analysis. Yield: 11.8 mg (11 % based on W)

IR (KBr): 1697 (s, $\nu_{C=O}$), 1607 (s, $\nu_{C=C}$), 1092 (s, $\nu_{W=O}$), 1036 (s, $\nu_{W=O}$), 962 (s, $\nu_{W=O}$), 916 (s, $\nu_{W=O}$), 818 (s, $\nu_{W=O}$) cm^{-1}. Elemental analysis; $C_{74}H_{125}K_3Mn_3N_{20}O_{149}P_8W_{34}$ calc. Mn 1.6, K 1.1, H 1.2, C 8.5, N 2.7; found Mn 1.5, K 1.2, H 1.2, C 8.5, N 2.9.

Methods

Single Crystal X-Ray Diffraction: SC-XRD measurements were performed on a Bruker SMART Apex II CCD diffractometer with Mo-Kα radiation ($\lambda = 0.71073$ Å). In each case, a suitable single crystal was removed from the mother liquor and mounted in Paratone® oil on a glass fibre and measured at 100 K under a stream of dry N_2. Structures were solved by direct methods and refined by a full-matrix least-squares technique on F^2 using SHELXTL.[3]

The PLATON SQUEEZE protocol was used to account for unassigned electron density in the crystal lattice associated with disordered solvent molecules which could not be modeled as discrete atomic positions.[4]

For compound **2**, approximately 48.2 % of the unit cell volume comprises a large region of disordered solvent that could not be modeled as discrete atomic sites. We employed PLATON SQUEEZE to calculate the contribution to the diffraction from the solvent/cation region and thereby produced a set of solvent-free diffraction intensities. SQUEEZE estimated a total count of 2993 electrons per unit cell which were assigned to 4 K^+, 8 C_4H_9O, 12 CH_3CN and 3 H_2O molecules per cluster.

For compound **3**, approximately 49.5 % of the unit cell volume or 3914 electrons per unit cell which were assigned to 4 K^+, 12 C_4H_9O, 18 CH_3CN and 3 H_2O molecules per cluster.

For compound **4**, approximately 54.6 % of the unit cell volume or 10083 electrons per unit cell which were assigned to 4 K^+, 12 C_4H_9NO, 120 CH_3CN and 40 H_2O molecules per cluster.

Electrochemical measurements were performed using a CHI Instruments electrochemical workstation equipped with a standard three-electrode arrangement; working electrode: glassy carbon (d = 3 mm), reference electrode: saturated calomel (SCE), and counter electrode: Pt wire. Cyclic voltammetry (CV) experiments were performed in dry dimethylformamide (DMF) using $n\mathrm{Bu_4NPF_6}$ (0.1 M) as a supporting electrolyte. All solutions were purged with nitrogen for at least 10 min to remove O_2 and kept under a positive pressure of N_2 while performing the experiment. Potentials are quoted vs NHE using a standard correction of +244 mV vs SCE.

Controlled potential absorption spectra were recorded using a Shimadzu UV-3150 spectrometer combined with an ALS BAS Model 620E potentiostat. A Pt mesh working electrode, Pt coil counter electrode and SCE reference electrode were used in combination with a specialized quartz spectro-electrochemical cell, incorporating a 0.5 mm cuvette fitted with rubber septums. The supporting electrolyte was 0.1 M $\mathrm{TBAPF_6}$. The stated potentials were applied until the solution reached an equilibrium state.

A Xe-lamp equipped with a cut-off filter at either $\lambda = 390$ nm or 420 nm was used as the light source during all photooxidation measurements. A fixed current of 5 amps was supplied by the power source during all experiments and it was ensured that all samples were placed equidistant (10 cm) to the irradiation point source in long-necked quartz cuvettes during each measurement. UV-Vis spectrometry was used to monitor the decrease in absorbance of the characteristic absorption band of indigo dye at 613 nm as a function of time.

Electrospray Ionisation Mass Spectrometry: ESI-MS measurements were performed on an AB SciEX Triple TOF 4600 spectrometer operating in negative mode. All samples were prepared to a concentration of 5×10^{-6} M in acetonitrile and introduced by direct injection via an integrated syringe pump at a constant flow rate of 5 μL min^{-1}. Source parameters were as follows: source voltage: 5.5 kV, source temperature: 150 °C, de-clustering potential: 25 V, collision energy: 10 V.

^{1}H and ^{31}P NMR: NMR spectra were measured on a Bruker AVANCE 400 spectrometer at room temperature. Chemical shifts are reported in ppm (δ) relative to the employed standard (^{1}H NMR: tetramethylsilane (TMS), ^{31}P NMR: H_3PO_4).

Absorption spectra were measured on a Shimadzu UV-3150 spectrometer in DMF. All measurements were performed in optically matched quartz cuvettes under air.

Fourier transform infra-red (FTIR) spectra were measured on a SHIMADZU IR Affinity-1 spectrometer, where samples were prepared as a KBr disc.

Elemental Analysis: Values for C, H and N content were obtained using a Perkin Elmer 2400 elemental analyser. K content was obtained by ICP-AES measurement using a Shimadzu ICP-8100 spectrometer.

Crystallography

Table S1: Crystallographic Details

	2	**3**	**4**
Chemical Formula	$C_{84}H_{174}K_4N_{20}O_{147}P_8W_{34}Zn$	$C_{112}H_{198}CoK_4N_{30}O_{151}P_8W_{34}$	$C_{280}H_{519}K_3Mn_3N_{123}O_{189}P_8W_{34}$
M_r (g mol^{-1})	10536.85	11094.98	15413.93
Crystal System	Monoclinic	Monoclinic	Orthorhombic
Space Group	P 21/c	P 21/c	$Pna2_1$
a (Å)	29.322(5)	29.492(4)	29.813(8)
b (Å)	19.862(3)	19.778(2)	24.940(7)
c (Å)	37.160(7)	37.459(5)	35.412(9)
α (°)	90.0	90.0	90.0
β (°)	102.943(3)	103.196(2)	90.0
γ (°)	90.0	90.0	90.0
V (Å^3)	21092(6)	21273(5)	26330(12)
Z	4	4	4
T (K)	100(2)	100(2)	100(2)
$F_{(000)}$	18944	20108	29360
$\rho_{calcd.}$ (g cm^{-3})	3.318	3.464	3.888
$\mu(Mo_{K\alpha})$ (mm^{-1})	18.812	18.630	15.192
Rflns. (measd.)	108373	105327	134219
Rflns. (uniq.)	41276 (R_{int} = 0.099)	38923(R_{int} = 0.235)	37780 (R_{int} = 0.343)
No. params.	996	1039	989
$R1$ ($I > 2\sigma(I)$)	0.1018	0.0968	0.0883
$wR2$ (all)	0.2667	0.2847	0.2995
S	1.327	0.936	0.888

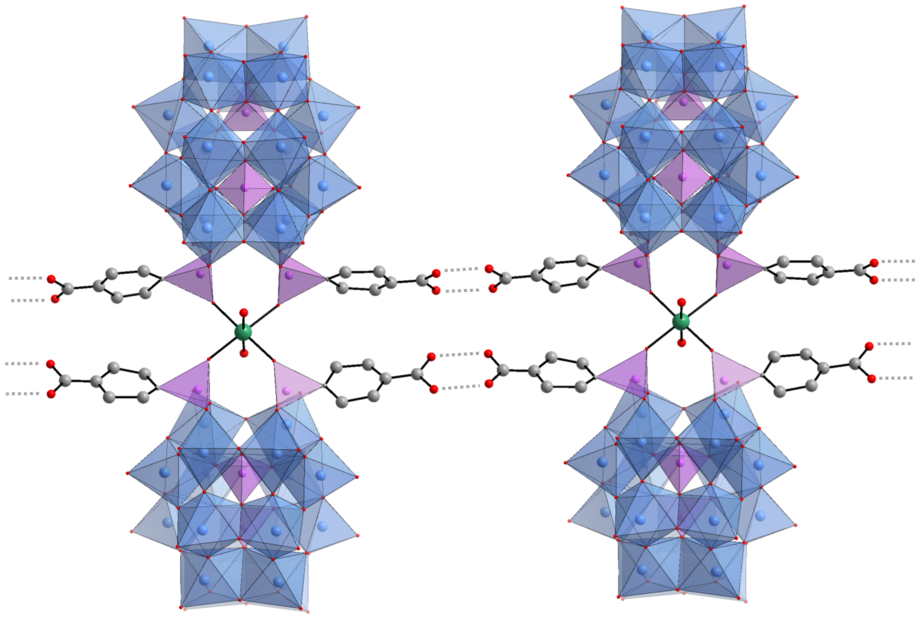

Figure S1. Hydrogen bonding interaction (d_{O-O} = 2.523 Å) between discrete clusters of **2** (or **3**), showing the formation of chain-like aggregates in the solid state and indicating protonation of the carboxylic acid groups. Colour code: blue polyhedra = {WO_6}, purple polyhedra = {PO_4} or {PO_3C}, green = Zn/Co, red = O, grey = C. Cations, protons and solvent molecules have been removed for clarity.

Mass Spectrometry

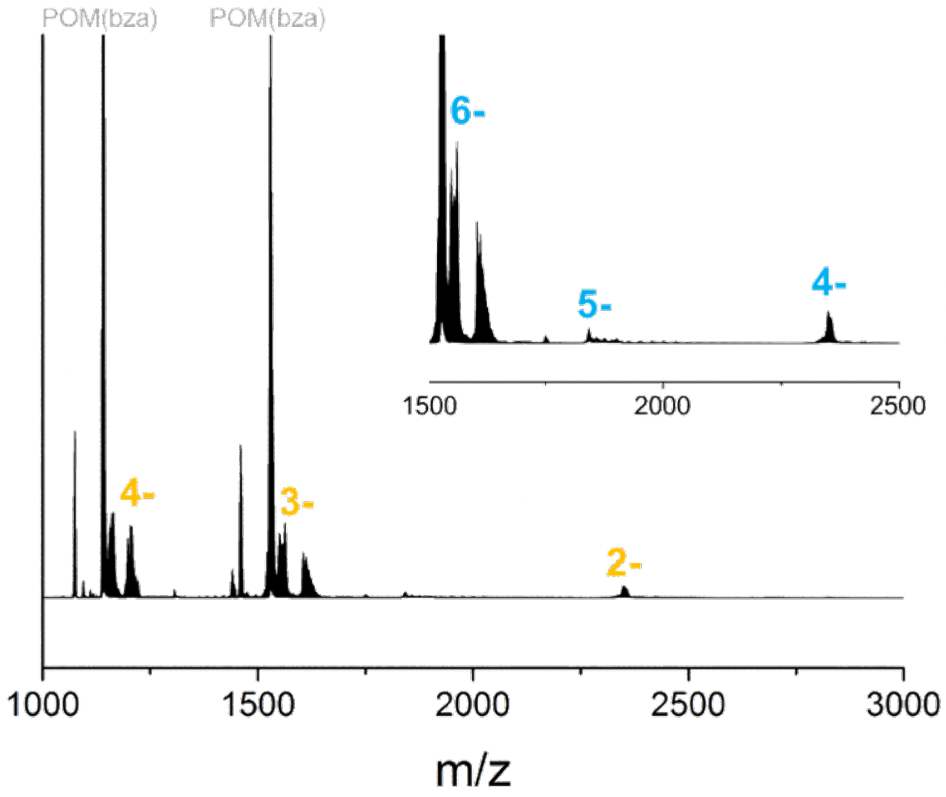

Figure S2. Negative mode ESI-MS spectrum of compound **2**. Inset shows location of higher mass species corresponding to the intact product. Note: 'POM(bza)' corresponds to compound **1**.

Table S2. Selected mass spectrometry peak assignments for compound **2**.

***m/z* (obs)**	***Z***	**Assignment**	***m/z* (calc)**
1530.0	6-	$\{K_2H_2[Zn(H_2O)_2(P_2W_{17}O_{57}(PO_5H_5C_7)_2)_2]\}$	1530.1
1841.7	5-	$\{NaH_4[Zn(H_2O)_2(P_2W_{17}O_{57}(PO_5H_5C_7)_2)_2].CH_3CN\}$	1841.7
1858.6	5-	$\{K_4H[Zn(H_2O)_2(P_2W_{17}O_{57}(PO_5H_5C_7)_2)_2].2H_2O\}$	1858.7
2352.1	4-	$\{K_4H_2[Zn(H_2O)_2(P_2W_{17}O_{57}(PO_5H_5C_7)_2)_2].CH_3CN.6H_2O\}$	2351.9
1198.3	4-	$\{KNa[Zn(H_2O)_2(OH)_2(P_2W_{17}O_{57}(PO_5H_5C_7)_2)].CH_3CN.3H_2O\}$	1198.0
1204.0	4-	$\{K_2Na[Zn(H_2O)(OH)_3(P_2W_{17}O_{57}(PO_5H_5C_7)_2)].2CH_3CN\}$	1204.2
1605.6	3-	$\{K_2Na[Zn(H_2O)_2(OH)_2(P_2W_{17}O_{57}(PO_5H_5C_7)_2)].2CH_3CN\}$	1605.9
2349.4	2-	$\{KNa[Zn(H_2O)_4(P_2W_{17}O_{57}(PO_5H_5C_7)_2)_2]\}$	2349.4
1140.7	4-	$\{Na_2[P_2W_{17}O_{57}(PO_5H_5C_7)_2].H_2O\}$	1140.7
1529.7	3-	$\{Na_2H[P_2W_{17}O_{57}(PO_5H_5C_7)_2].CH_3CN\}$	1528.9

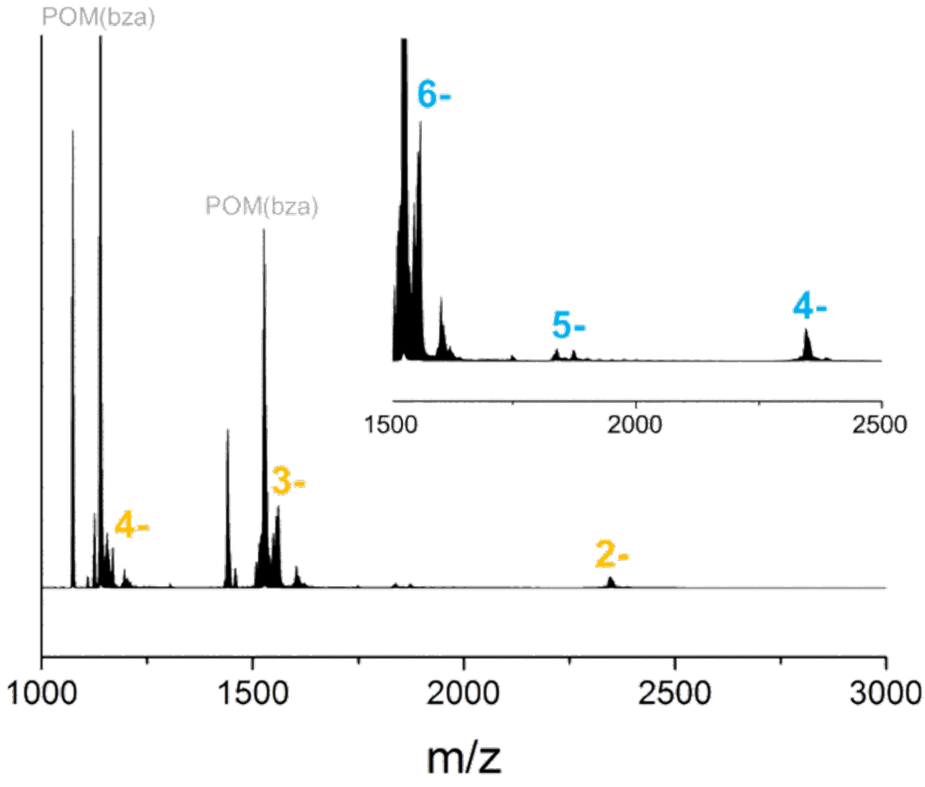

Figure S3. Negative mode ESI-MS spectrum of compound **3**. Inset shows location of higher mass species corresponding to the intact product. Note: 'POM(bza)' corresponds to compound **1**.

Table S3. Selected mass spectrometry peak assignments for compound **3**.

***m/z* (obs)**	***Z***	**Assignment**	***m/z* (calc)**
1528.1	6-	$\{H_4[Co(H_2O)_2(P_2W_{17}O_{57}(PO_5H_5C_7)_2)_2].4H_2O\}$	1528.3
1832.2	5-	$\{Na_2H_3[Co(H_2O)_2(P_2W_{17}O_{57}(PO_5H_5C_7)_2)_2].H_2O\}$	1832.1
1873.3	5-	$\{K_3H_2[Co(H_2O)_2(P_2W_{17}O_{57}(PO_5H_5C_7)_2)_2].2CH_3CN.4H_2O\}$	1873.3
2348.6	4-	$\{K_4H_2[Co(H_2O)_2(P_2W_{17}O_{57}(PO_5H_5C_7)_2)_2].3CH_3CN.H_2O\}$	2348.4
2367.4	4-	$\{K_6[Co(H_2O)_2(P_2W_{17}O_{57}(PO_5H_5C_7)_2)_2].3CH_3CN.H_2O\}$	2367.4
1196.8	4-	$\{K_2Na[Co(H_2O)(OH)_3(P_2W_{17}O_{57}(PO_5H_5C_7)_2)].CH_3CN.H_2O\}$	1196.9
1203.0	4-	$\{KNa_2[Co(H_2O)(OH)_3(P_2W_{17}O_{57}(PO_5H_5C_7)_2)].2CH_3CN.H_2O\}$	1203.2
1603.3	3-	$\{KNaH[Co(H_2O)_2(OH)_2(P_2W_{17}O_{57}(PO_5H_5C_7)_2)].2CH_3CN.2H_2O\}$	1603.3
2345.9	2-	$\{KNa[Co(H_2O)_4(P_2W_{17}O_{57}(PO_5H_5C_7)_2)_2]\}$	2345.9
1125.2	4-	$\{H_2[P_2W_{17}O_{57}(PO_5H_5C_7)_2]\}$	1125.2
1526.9	3-	$\{KNaH[P_2W_{17}O_{57}(PO_5H_5C_7)_2].H_2O\}$	1529.6

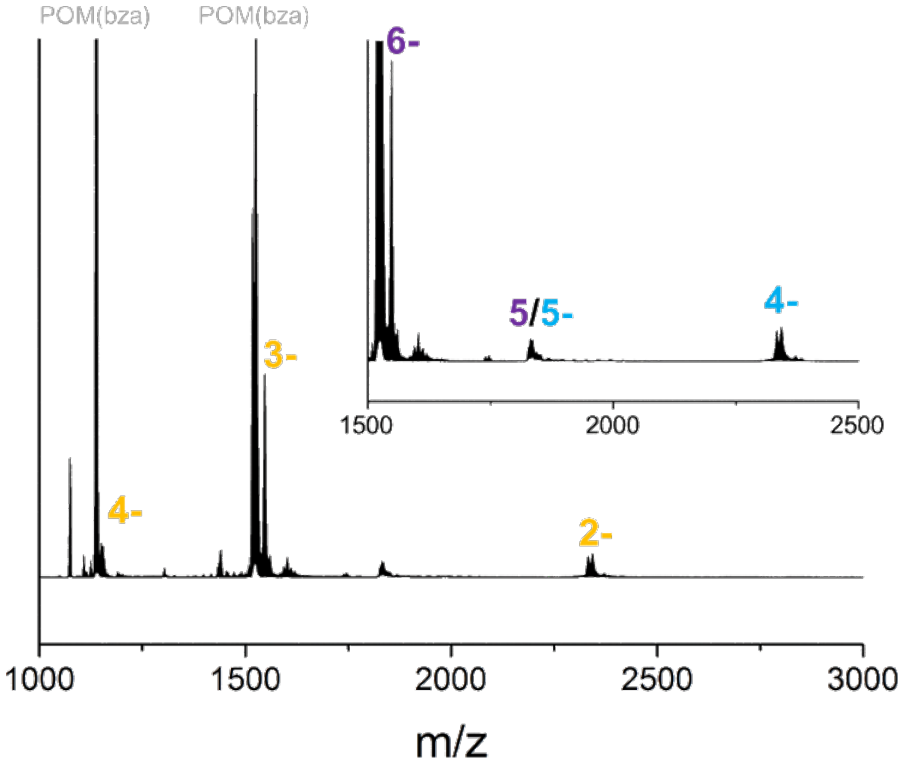

Figure S4. Negative mode ESI-MS spectrum of compound **4**. Inset shows location of higher mass species corresponding to both the intact product (blue) and the mono-manganese fragment (purple), potentially corresponding to the structural type observed in compounds **2** and **3**. Note: 'POM(bza)' corresponds to compound **1**.

Table S4. Selected mass spectrometry peak assignments for compound **4**

m/z (obs)	*Z*	Assignment	*m/z* (calc)
1851.2	5-	$\{H_5[Mn_2(OH)_2(H_2O)_4(P_2W_{17}O_{57}(PO_5H_5C_7)_2)_2].2H_2O\}$	1851.1
1868.4	5-	$\{H_5[Mn_2(OH)_2(H_2O)_4(P_2W_{17}O_{57}(PO_5H_5C_7)_2)_2].3CH_3CN\}$	1868.5
2339.0	4-	$\{K_2H_4[Mn_2(OH)_2(H_2O)_4(P_2W_{17}O_{57}(PO_5H_5C_7)_2)_2].CH_3CN.H_2O\}$	2338.9
1522.0	6-	$\{H_4[Mn(H_2O)_2(P_2W_{17}O_{57}(PO_5H_5C_7)_2)_2].CH_3CN\}$	1522.4
1831.5	5-	$\{Na_2H_3[Mn(H_2O)_2(P_2W_{17}O_{57}(PO_5H_5C_7)_2)_2].H_2O\}$	1831.3
1842.6	5-	$\{KNa_2H_2[Mn(H_2O)_2(P_2W_{17}O_{57}(PO_5H_5C_7)_2)_2].2H_2O\}$	1842.5
1190.3	4-	$\{K_2[Mn(H_2O)_2(OH)_2(P_2W_{17}O_{57}(PO_5H_5C_7)_2)].CH_3CN.H_2O\}$	1190.4
1602.4	3-	$\{K_2Na[Mn(H_2O)_2(OH)_2(P_2W_{17}O_{57}(PO_5H_5C_7)_2)].2CH_3CN\}$	1602.6
2343.4	2-	$\{KNa[Mn(H_2O)_3(OH)(P_2W_{17}O_{57}(PO_5H_5C_7)_2)_2]\}$	2343.4
1138.5	4-	$\{H_2[P_2W_{17}O_{57}(PO_5H_5C_7)_2].3H_2O\}$	1138.7
1525.9	3-	$\{NaH_2[P_2W_{17}O_{57}(PO_5H_5C_7)_2].3H_2O\}$	1525.9

Electrochemistry

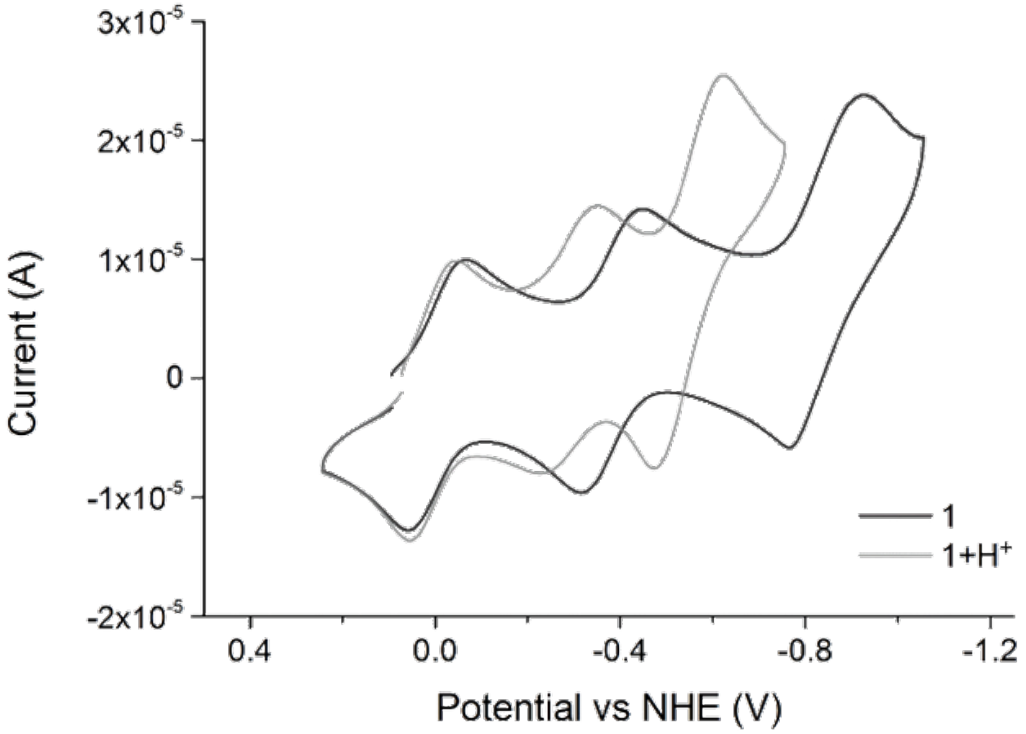

Figure S5. Cyclic voltammetry of **1** (black) and **1** in the presence of 1000 equivalents of CH_3COOH (grey) showing the positive potential shift of the 2nd and 3rd redox waves (see Table 2), which indicated proton-coupled electron transfer behaviour in the presence of a proton-donor. Conditions: 0.1 mM compound **1**, 1 mM $TBAPF_6$, solvent = DMF, scan rate = 0.1 V s^{-1}. Both CVs were initially scanned from the open circuit potential in the negative direction.

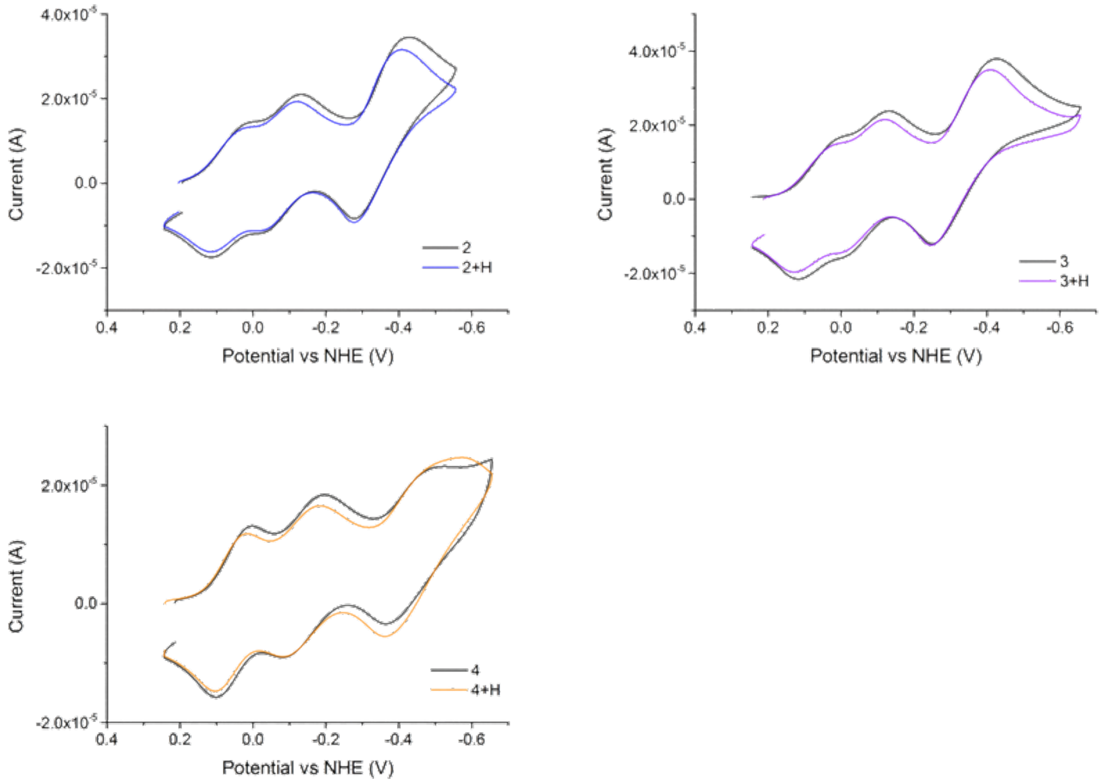

Figure S6. Cyclic voltammetry of compounds **2**-**4** (black) and when measured in the presence of 1000 equivalents of CH_3COOH (coloured) showing that, in contrast to the behaviour of compound **1**, no significant potential shifts are observed in the presence of additional protons. This indicates that the metal-functionalised hybrid clusters do not undergo proton-coupled electron transfer, unlike the parent compound **1**. Conditions: 0.1 mM compound **2**-**4**, 1 mM $TBAPF_6$, solvent = DMF, scan rate = 0.1 V s^{-1}. All CVs were initially scanned from the open circuit potential in the negative direction.

Spectroelectrochemistry

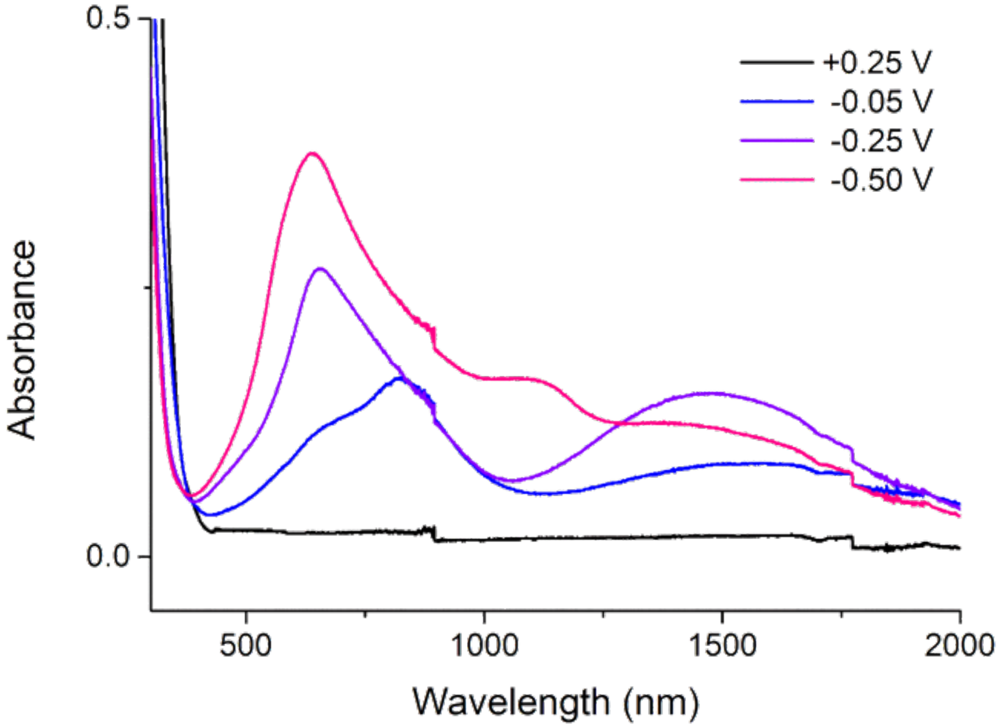

Figure S7. Controlled potential UV-vis spectroscopy of **2**, showing the growth of both IVCT (in the visible and near-IR regions, respectively), as a representative example of the behaviour of each of the metal-functionalised hybrid clusters **2-4**. The first reduction (at -0.05 V vs NHE) has a characteristic wavelength in the visible region of *ca.* 830 nm, the second at *ca.* 660 nm and the third at *ca.* 635 nm (with an additional peak appearing at *ca.* 1100 nm in the near-IR).

Photochemistry

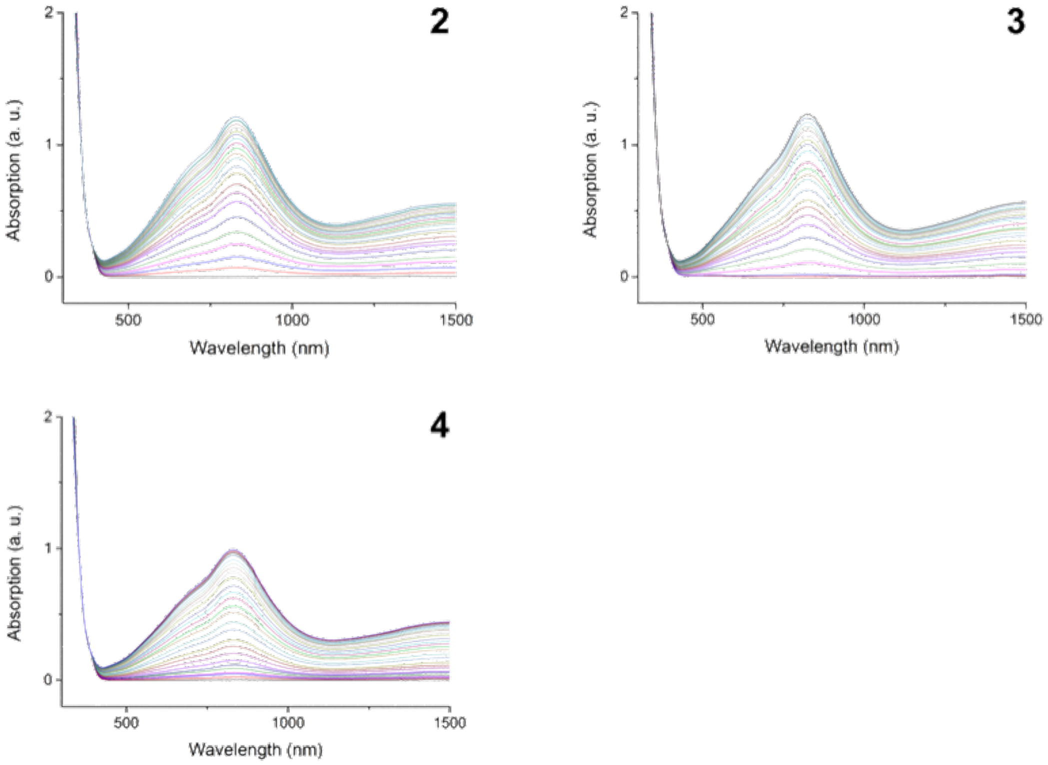

Figure S8. UV-vis spectra showing the photoreduction and 1e$^-$ charge accumulation on compounds **2-5** under irradiation by a Xe light source (λ > 420 nm) in strictly degassed DMF. The maxima at 830 nm corresponds to the IVCT band of the singly reduced polyoxometalate cluster as determined by controlled potential UV-Vis spectroscopy (see Figure S7). All spectra show data collected at 2-minute intervals over 60 minutes of irradiation.

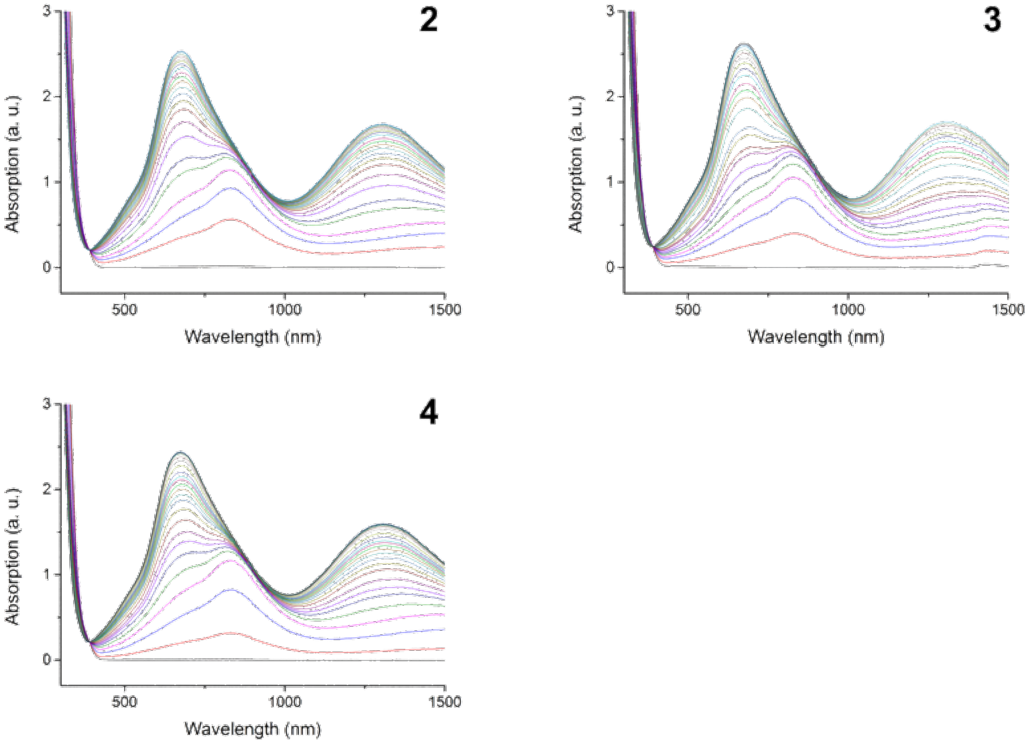

Figure S9. UV-vis spectra showing the photoreduction and $2e^-$ charge accumulation on compounds **2**-**4** under irradiation by a Xe light source ($\lambda > 390$ nm) in strictly degassed DMF. The maxima at 830 nm and ca. 660 nm in the visible region correspond to the IVCT bands of the singly and doubly reduced polyoxometalate clusters, respectively, as determined by controlled potential UV-Vis spectroscopy (see Figure S7). All spectra show data collected at 2 minute intervals over 60 minutes of irradiation.

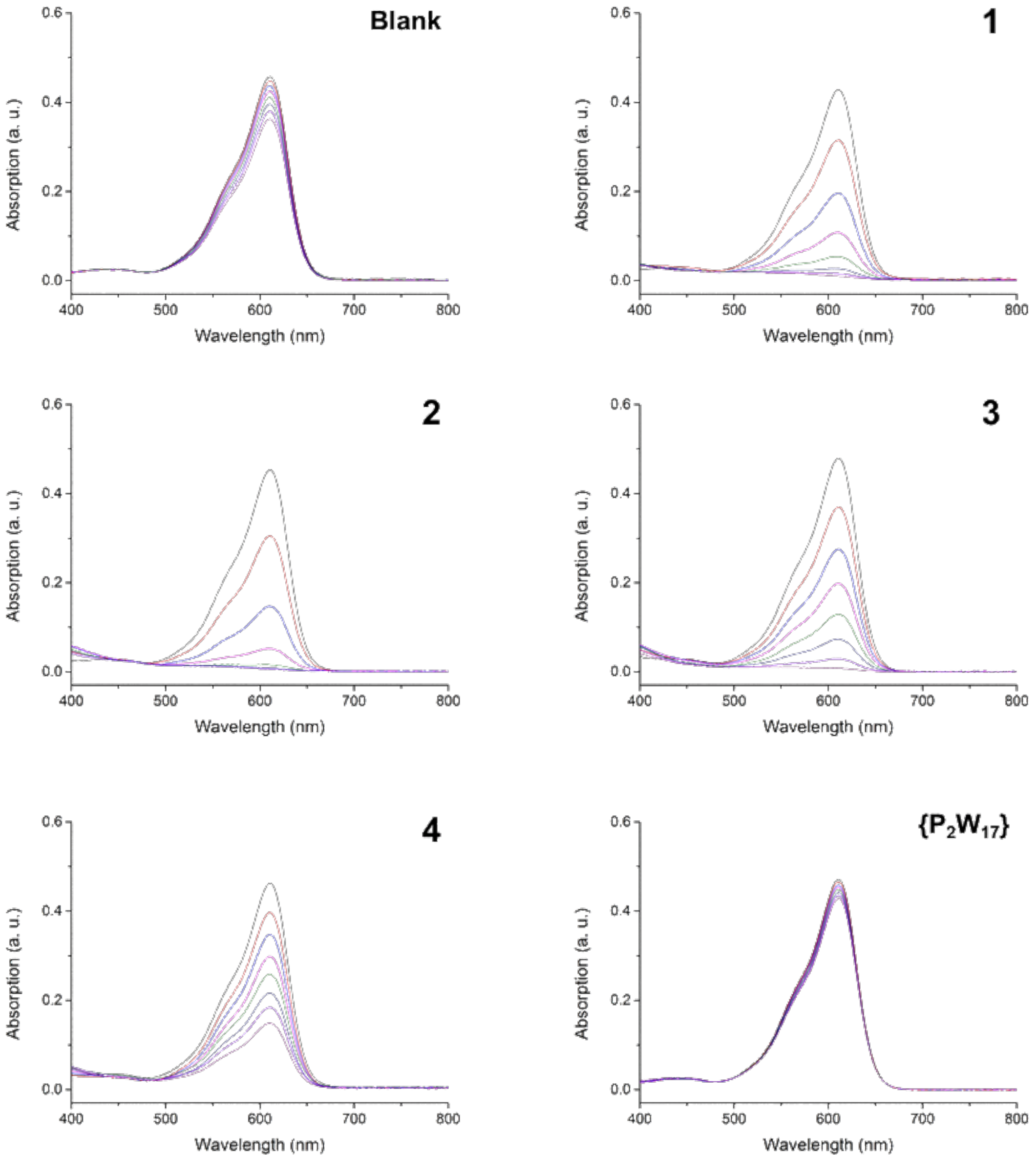

Figure S10. UV-Vis spectra showing the photo-oxidative decomposition of indigo dye in the presence of compounds **1-5**, $\{P_2W_{17}\}$ and a control reaction containing no catalyst. All spectra show data collected from 0 to 80 minutes at 10 minute intervals (λ > 390 nm).

UV-Vis Spectroscopy

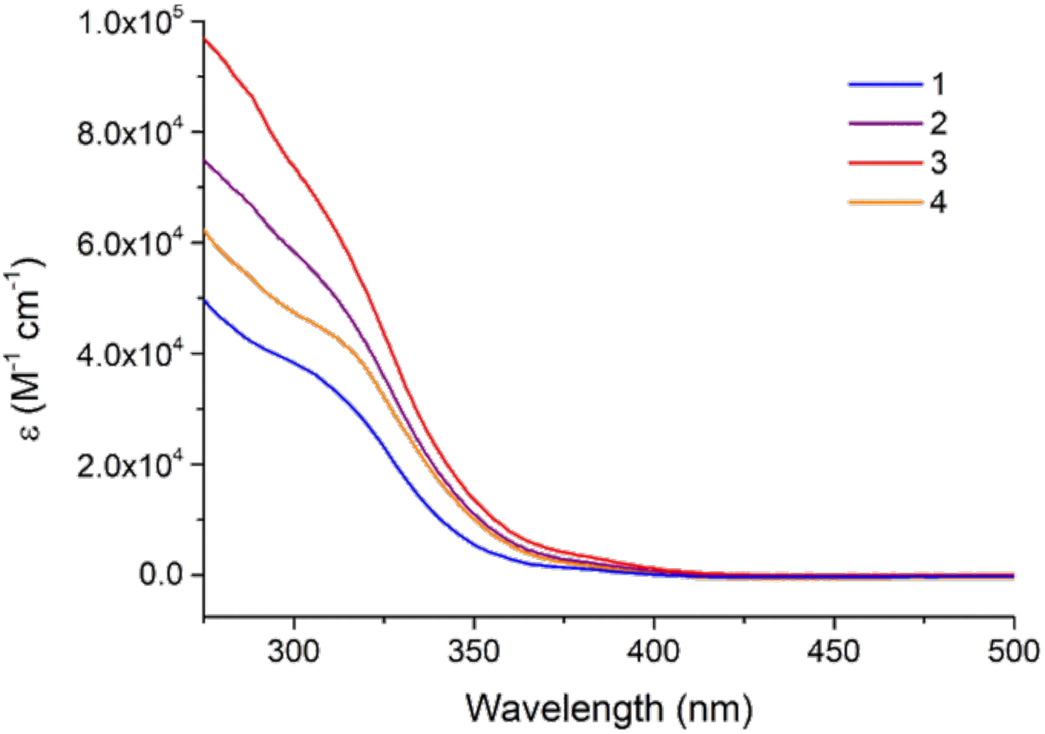

Figure S11. UV-Vis spectroscopy of compounds **1** – **4** measured in *N,N'*-Dimethylformamide.

References

[1] M. Sasmita and P. Panchanan, *Colloids Surf. A.*, 2009, **339**, 35–42.

[2] Cameron, J. M.; Fujimoto, S.; Kastner, K.; Wei, R.-J.; Robinson, D.; Sans, V.; Newton, G. N.; Oshio, H. Orbital Engineering: Photoactivation of an Organofunctionalized Polyoxotungstate. *Chem. Eur. J.,* 2017, **23**, 47.

[3] G. Sheldrick, *Acta Crystallogr., Sect. A: Found. Crystallogr.*, 2008, **64**, 112-122.

[4] A. L. Spek, *Acta Crystallogr. Sect. C-Struct. Chem.* 2015, **71**, 9.